

Reactive electron beam evaporation of gadolinium oxide optical thin films for ultraviolet and deep ultraviolet laser wavelengths

N.K. Sahoo*, S. Thakur, M. Senthilkumar, D. Bhattacharyya, N.C. Das

Spectroscopy Division, Bhabha Atomic Research Centre, Trombay, Mumbai 400 085, India

Received 23 August 2002; received in revised form 17 March 2003; accepted 14 April 2003

Abstract

Availability of ultraviolet optical thin film materials, especially high index refractory oxides that transmit down to deep ultraviolet (approx. 0.2 μm) is very much limited. The present article discusses some of the research optimization studies on gadolinium oxide (Gd_2O_3), a novel lanthanide sesquioxide material, for such challenging spectral requirements. Optical and topographical properties of single layer films have been studied using phase modulated spectroscopic ellipsometry, spectrophotometry and multimode atomic force microscopy. Films deposited at lower substrate temperatures have shown higher band gaps and higher substrate temperatures yielded higher refractive indices. Multilayer high reflection filters have been developed for ultraviolet laser wavelengths such as ArF (193 nm), KrCl (222 nm), KrF (248 nm) and Nd-Yag-III (355 nm), using this material at lower substrate temperature conditions and successfully tested for their performances.

© 2003 Elsevier Science B.V. All rights reserved.

Keywords: Atomic force microscopy; Optical coating; Optical properties; Surface morphology; Multilayers; Ellipsometry; Gadolinium oxide; Microstructural properties; Viscoelastic property; Force modulation; E-beam evaporation

1. Introduction

One of the most important regions of the electromagnetic spectra, which represents state-of-the-art in both lasers and coatings are the ultraviolet (UV) from 0.2 to 0.35 μm . There are very few thin film materials with suitable optical and mechanical properties which can satisfy the coating requirements in this wavelength region. Most of the coating materials, which are transparent in the visible region, become highly absorbing in the UV region. Thus, this spectral region has been posing considerable challenges with respect to new materials and their combinations. There are a few UV-transmitting high index materials-like Al_2O_3 , HfO_2 , Sc_2O_3 and ceramic composites, which have been tried out by several thin film experimentalists for developing multilayer optical coatings [1–5]. However, most of the research studies have indicated that such materials form a durable coating only when deposited at higher substrate temperatures. In the course of our present optimization studies, Gadolinium oxide is found to be a

potential candidate for such requirements with its transmitting region starting approximately near 0.19 μm and extending beyond 16 μm . This makes it an attractive high index optical film material not only for ultraviolet coatings but also for multilayer devices with extended spectral characteristics for lasers and related applications. This novel material also forms durable coatings even when deposited at ambient substrate temperatures, which makes it as an attractive choice for a variety of substrates and low index coating materials for developing multilayers.

Technologically, UV-laser coatings and materials have applications in laser ablation, laser spectroscopy, fluorescence stimulation in bio-medical applications and more recently, in photolithography of ever-decreasing dimensions in microprocessor manufacturing. Typical laser wavelengths for such applications include 355 and 266 nm (third and fourth harmonics of Nd-YAG), 351 nm (XeF), 308 nm (XeCl), 248 nm (KrF), 222 nm (KrCl) and 193 nm (ArF). The shorter wavelengths belonging to excimer gas lasers have applications in deep UV microlithography for generating feature sizes <0.25 μm for data storage and microelectronics fabri-

*Corresponding author. Fax: +91-22-5505151.

E-mail address: nksahoo@apsara.barc.ernet.in (N.K. Sahoo).

cation. Most importantly, the pulse widths for excimer lasers vary from ~ 30 ns to sub-ns with powers exceeding 500 MW and repetition rates approaching 1 kHz. For such specific high power laser applications laser induced damage has also been putting additional limiting factors and constraints [3]. This necessitates having designs and coating materials with maximum stability at such high laser powers. In this work, process parametric studies of a novel thin film optical coating material using gadolinium oxide (Gd_2O_3), a lanthanide sesquioxide, as a high index material are reported. Some advanced characterization techniques such as phase modulated spectroscopic ellipsometry, multimode scanning-probe microscopy and uv–vis-nir spectrophotometry has been used in investigating optical and microstructural properties of the electron beam deposited films. Some multilayer devices for ultraviolet lasers such as ArF (193 nm), KrCl (222 nm), KrF (248 nm), XeF (351 nm) and Nd-Yag-III (355 nm) have been successfully developed and tested using this novel material along with SiO_2 as the low index counterpart.

2. Previous studies on gadolinium oxide

Gadolinium oxide (Gd_2O_3) has in recent days drawn considerable attention in microelectronics, magnetic recording media, new superconducting components, and semiconductor and optoelectronic technologies. GdO_x has been found to produce layers with excellent surface morphologies as evidenced by surface roughness of less than 1 nm. Both good interfacial electrical characteristics and good thermal stability of Gadolinium oxide are being utilized for reproducible fabrication of high performance metal oxide semiconductor field effect transistors (MOSFETs) from compound semiconductors [6,7]. Gd_2O_3 is one of the prominent rare earth oxides used to stabilize ZrO_2 because its cubic phase appears at a lower dopant content [8]. Steiner et al. [9] have studied, epitaxially grown crystalline Gd_2O_3 on GaAs substrate and its structural modifications with heat exposures and mild ion bombardment [9]. Like most other lanthanide sesquioxide single crystals, Gd_2O_3 crystallizes in monoclinic, hexagonal and cubic structures [9]. García-Murillo et al. have recently studied some of the optical and structural aspects of the films prepared by the sol-gel technique for high-resolution X-ray imaging applications [10]. It is well known that the resolution in such imaging applications can be improved using a thin and dense scintillating film. Therefore, their primary aim was to produce a highly dense lanthanide sesquioxide Ln_2O_3 ($Ln=Gd, Lu$) with good scintillation performances and they observed Gd_2O_3 to be the most appropriate candidate.

Recently, Dakhel has reported some of the optical properties of Gd_2O_3 films, prepared by evaporation from resistively heated crucible in the wavelength region of

300–700 nm [11]. He observed that the amorphous structure for his film of approximately 180 nm thicknesses and also predicted its band gap to be more than 6 eV. In spite of several attractive properties of such a high band gap lanthanide sesquioxide material, there is no such detailed process optimization study reported so far related to optical coating applications, which is the prime objective of our present investigations.

3. Experimental aspects

The gadolinium oxide films have been evaporated by reactive electron beam evaporation using VERA 902 automated optical coating system. The gadolinium oxide granules of Cerac's product-G-1076 with the purity $>99.9\%$ have been used for this thin film evaporation. The real time rate of deposition and total physical thickness were controlled and determined by Leybold's XTC/2 quartz crystal monitors. A residual gas analyzer of Pfeiffer's Prisma 200 has been used to analyze the partial pressure of reacting gases. Leybold's OMS 2000 optical monitoring system has been used to record the optical thickness using quarterwave-monitoring approach. For controlling the total pressure during the reactive evaporation process, MKS mass flow controllers have been suitably interfaced with the coating system. More than 20 samples with various process parameters have been prepared for the present investigations. The optical transmittance and reflectance spectra of each film were recorded using Shimadzu's UV-3101PC uv–vis-nir spectrophotometer as well as Cary 2390 spectrophotometer systems (wavelength range: 185–3150 nm). The former spectrophotometric system uses an integrating sphere for determination of both specular and diffused reflectance characteristics of thin film samples. Subsequently, the samples were analyzed using phase modulated spectroscopic ellipsometric technique with the help of Jobin Yvon's UVSEL Ellipsometer (wavelength range: 175–1700 nm). The description of this system has been discussed elsewhere [12,13]. It is well known that most often the optical and physical properties of the films vary along the growth direction in a very complex manner. For such films spectrophotometric and ellipsometric measurements, yield a very different kind of spectral characteristics as compared to simplified and ideal homogeneous structures. Various realistic thin film-modeling approaches have been adopted to extract the dispersive optical constants, void fractions, surface roughness and physical thickness of such films [14,15]. Topographic and surface viscoelasticity measurements were carried out using a multimode scanning probe microscope of NT-MDT's Solver P-47H. The details of these measurements and analyses are presented in the subsequent sections.

4. Analysis by phase modulated ellipsometry (PME)

During the last few years, it is well known amongst the thin film researchers that the PME technique can be conveniently extended to non-destructively detect and characterize the distribution of inhomogeneities in transparent or weakly absorbing films, interfaces and can also determine the optical function of the film material at the same time [16]. Essential parameters of a slightly inhomogeneous thin film are the mean dispersive refractive index, physical thickness and the degree of inhomogeneity [17]. An important role in the theoretical analysis of spectroscopic ellipsometric data is played by the so-called, quarter-wave (QW) and half-wave (HW) wavelength points [18]. The consideration of films with linear refractive-index profiles predicts that the values of the ellipsometric angle Ψ at the QW points are independent of the degree of inhomogeneity, whereas those values at the HW points are most sensitive to the film inhomogeneities and can be used to determine the degree of the inhomogeneity. This approximation is based on the assumption that the contribution of the interference effect inside the film can be ignored. At the same time, it incorporates exactly the reflections connected with abrupt changes of the refractive index profiles at the film boundaries. This approximation, however, is only a first approximation to the properties of inhomogeneous films. It is valid for films with a linear refractive index profile, but it does not entirely fit with the properties of ellipsometric spectra in the case of complicated refractive index profiles. Subsequently, it has been demonstrated that the ψ values at the QW points are independent of film inhomogeneity in only some of the special cases. Charmet and Gennes later derived a more precise approximation for the case of inhomogeneous layer bounded by the interface with homogeneous substrate [19]. In this case, the effect of the interface was incorporated exactly, whereas for the inhomogeneous layer the first Born approximation was used. Such an approach was later extended to include the local perturbations at both sides of the substrate. Subsequently, Tikhonravov and coworkers derived a more precise approximation for the inhomogeneous film with two abrupt changes of the refractive index at the substrate and the ambient interfaces [20,21].

During the present investigation, spectroscopic phase modulated ellipsometric technique has been extensively used to characterize the thin films for their refractive index, extinction coefficient, physical thickness and relative compositions. Since some of the present films showed index non-linearity in their characteristics, such behaviour was modeled using discrete-layer-based analysis techniques. Among others, the roughness of surfaces or interfaces has long been known to influence the ellipsometric data, and many groups have investigated this issue both theoretically and experimentally. It is

widely believed today that the effect of surface roughness on ellipsometric measurement can be quantitatively simulated by treating the roughness as an imaginary layer and can be involved in the theory of effective medium approximations [22]. The effective medium approximation (EMA) is mostly accepted as a standard procedure for treating mixed thin film layers including physical roughness in the optical analysis, when it is assumed, the lateral characteristic length of the roughness is much smaller than the wavelength. Recent sophisticated use of EMA has shown to be capable of implicitly taking into account of the specific surface structures with defined distance and radius [22]. The general equation that describes the optical properties of the mixture of m materials in EMA is given as follows:

$$\frac{\varepsilon - \varepsilon_h}{\varepsilon + K \varepsilon_h} = \sum_{j=1}^m f_j \frac{\varepsilon_j - \varepsilon_h}{\varepsilon_j + K \varepsilon_h} \quad (1)$$

where ε_j and f_j are the dielectric function and volume fraction of phase j . The quantity ε_h is the dielectric function of the host material that has to be defined choosing one of EMA sub-models. K is the screening/depolarization factor and it is used to describe the microstructure of the mixtures in the material. For spherical inclusions, K takes the value of 2, which is the case for the gadolinium thin film samples used under present investigations. The topographical measurements of such samples using AFM technique have confirmed such compositional modeling.

It is always more convenient to analyze the inhomogeneity of a layer by transforming it into a multilayer sub-structure composed of many thin homogeneous layers of different dispersive refractive indices. The accuracy of this technique depends on the number of appropriate sub-layers with related index variation. Sometimes it is also possible to approximate the characteristics of such multilayer thin film systems to a continuously varying inhomogeneous index profile. During the present studies, we have adopted this approach for a qualitative as well as quantitative analysis of the structural as well as optical inhomogeneities in thin films [23]. These analyses have been carried out using three sub-layer systems with distinct optical and structural properties, which are very similar to the model proposed by Chindaudom et al. [24]. The dispersion for refractive indices as well as extinction coefficients has been defined for each sub-layer with the appropriate functions. As shown in Fig. 1, the model consists of a substrate film interface layer with some voids (thickness d_1 , void fractions vf_1), below a nearly void-free middle layer (thickness d_2 , void fractions vf_2) and a micro-rough surface dense over layer (thickness d_3 , void fractions vf_3). The optical constants have been suitably fitted using Cauchy's absorbent and transparent dispersion models in the appropriate spectral region of the

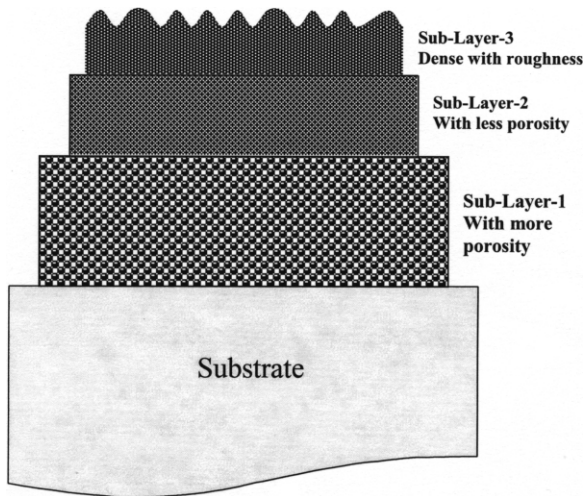


Fig. 1. Three-layer model of cross-section of thin film showing growth features and it has been used for the present phase modulated spectroscopic ellipsometric analysis.

measurement. The generalized form, which has been used during this work for the refractive index n and absorption coefficient k , is given by:

$$n(\lambda) = A + \frac{B \times 10^4}{\lambda^2} + \frac{C \times 10^9}{\lambda^4} \quad (2)$$

and,

$$k(\lambda) = D \times 10^{-5} + \frac{E \times 10^4}{\lambda^2} + \frac{F \times 10^9}{\lambda^4} \quad (3)$$

where λ is the wavelength in nm and A, B, C, D, E, F are coefficients for fitting. The ellipsometric spectra (ψ and Δ) of each sample are allowed to fit on basis of this model [25].

During the analysis and optimization it was observed that the three-layer growth models of most of the process-optimized samples converged to a two-layer structure and the thickness of the rough surface overlayer closely matches with the AFM measurements. Such a two-layer convergence has indicated a fairly homogeneous structure in these optimized films, which have been subsequently used for our multilayer development experiments. Some of the sample fittings in the ellipsometric data for the gadolinium oxide films have been shown in the Fig. 2a and b.

In the Fig. 2a fitting of ellipsometric parameters ψ and Δ have been depicted with both experimental and simulated characteristics. Fig. 2b depicts index dispersion of individual sub-layers used in the ellipsometric growth modeling of this sample. It is worth mentioning that for this measurement the single layer modeling could not be fitted to the ellipsometric spectral data within the acceptable tolerance value, since each film

has at least a roughness component. Although three-layer model has fitted our data reasonably well, there is a further scope of improving the results by incorporating more number of sub-layers in the modeling, which can lead to a more detailed structure. After the sub-layer growth analysis, the mean optical constants were computed in order to compare the variation in properties with respect to process parameters [23].

4.1. Deposition parameter dependence of refractive index

The deposition parameters for PVD processes that require close controls are: oxygen partial pressure, rate of deposition and substrate temperature. Conventionally, electron beam and resistance heated evaporation processes require optimized values in these parameters to achieve a high and desired quality thin film structure and properties. Like most thin films refractory oxide materials, optical properties of Gd_2O_3 have a strong dependency on these process parameters used during the present electron beam deposition process. The parametric dependences were systematically studied by varying a particular parameter, while keeping all others constant. In the present studies, it has been observed that the oxygen and substrate temperature are two dominant parameters in comparison to rate of deposition as presented below. Substantial differences in the optical properties have been observed in the samples prepared at ambient and elevated substrate temperatures. The most significant observation is the stable structure in the single layer thin films as well as multilayer devices developed at lower and even at ambient substrate temperatures. It opens up a wide range of possibilities for this well-behaved high index lanthanide sesquioxide film material in using it with varieties of substrate materials.

4.1.1. Substrate temperature dependence

Substrate temperature has played a very prominent role in controlling the mean refractive index and band gap of the present Gd_2O_3 films. Variation of spectral index profile with respect to temperature has been depicted in the Fig. 3. As it can be seen from this plot that the refractive index profile has a steady increase in their values as the substrate temperature increases. The highest temperature is restricted to 350 °C in considering the practical aspects of the deposition system. Most of the commercial coating systems like our present one (VERA 902) have the limitation in going beyond this temperature value. With this maximum limit to temperature, influence of other parameters for these films has been studied in detail. Most interestingly, the coatings at lower substrate temperatures those including the ambient have shown most promising results with respect to stability. Such a property will make these films more attractive in developing coatings on polymers, metal-dielectric filters and several other applications where

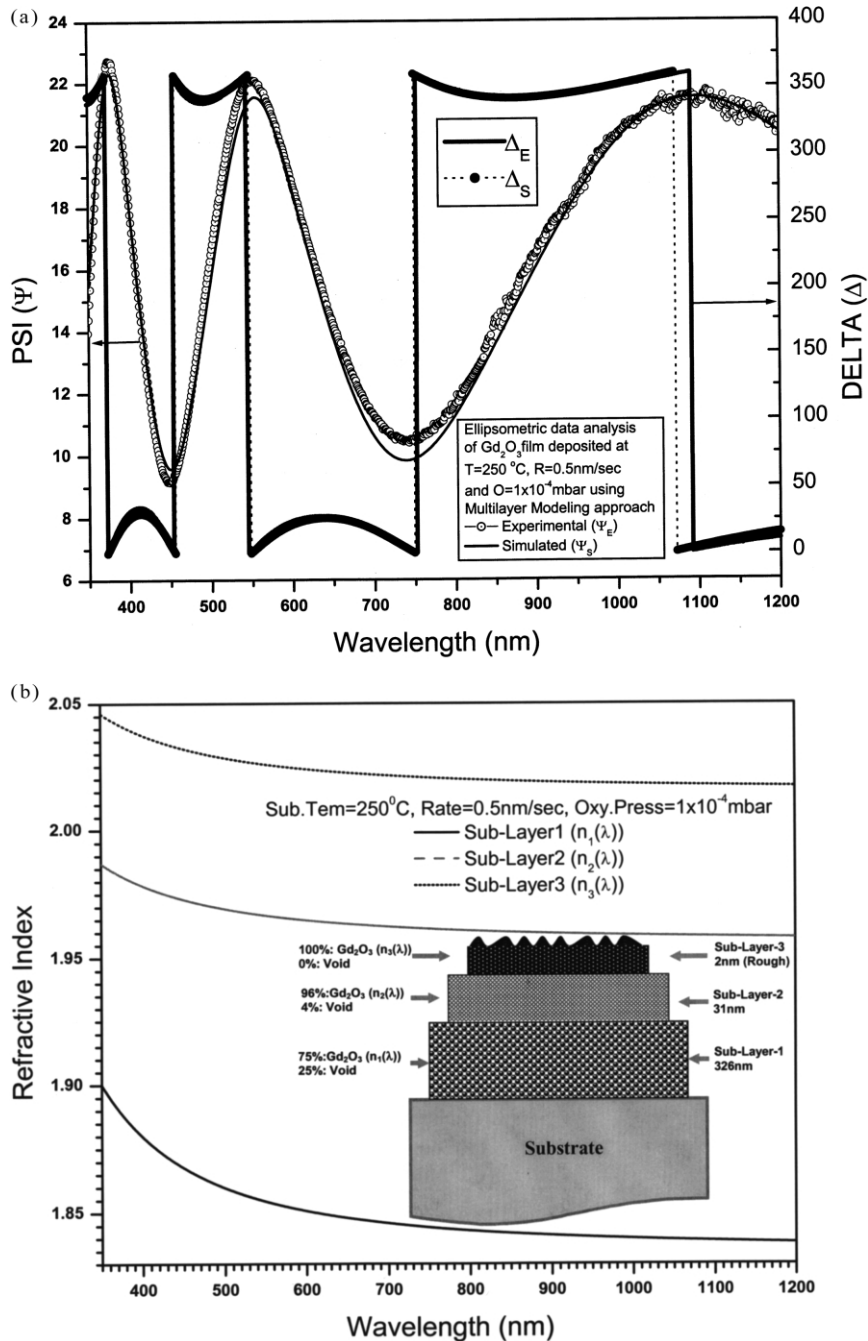


Fig. 2. (a) Spectroscopic ellipsometric analysis of Gd₂O₃ film using three layer model and (b) Corresponding computed refractive index variation. In this plot ψ_E, Δ_E are experimental values and ψ_S, Δ_S are simulated ellipsometric parameters.

room temperature conditions are required. In our present study, several high reflection filters have been developed for various ultraviolet and deep ultraviolet laser systems and the developmental task has been carried out at an ambient and low-substrate temperature conditions.

4.1.2. Oxygen pressure dependence

Oxygen pressure has very distinctive influences at different rate of depositions. The film deposited with rate of deposition of 1 nm/s, optimum oxygen pressure

of 1×10^{-4} mbar has produced the maximum value in the refractive index. Below and above this pressure it produces lower index profile as shown in the Fig. 4a and b. At a lower rate of 0.5 nm/s the extent of variation is relatively less as shown in Fig. 4a. In this figure, the variation of oxygen pressure has been shown for two extreme values. Similarly in Fig. 4b this variation is recorded for the rate of evaporation of 1 nm/s. It can be seen from this plot that the films deposited at 1×10^{-4} mbar have shown better spectral profile.

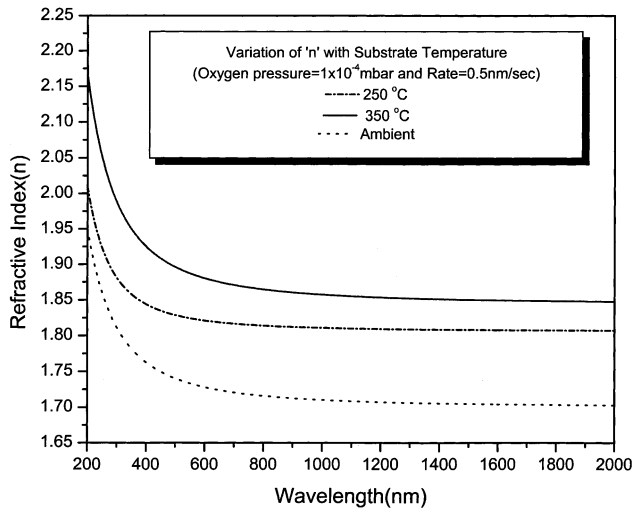


Fig. 3. Spectral variation of refractive index with respect to the substrate temperature. The deposition rate and oxygen pressures were maintained at 0.5 nm/s and 1×10^{-4} mbar, respectively, during this experiment.

4.1.3. Rate dependence

Rate of deposition has also different influences on refractive index at different substrate temperatures. In our experiment, the deposition rate has been varied from 0.5 to 2.0 nm/s at different substrate temperatures and oxygen pressures. It has been observed that at ambient substrate temperatures the variation in the rate of deposition has an opposite trend on the refractive index profile than at elevated temperatures. Fig. 5a and b have shown the variation of spectral index profile with respect to rate of deposition under two different substrate temperatures. It has been clearly noticed that ambient temperatures at lower rates give rise to higher spectral index where as the effect is opposite at higher substrate temperature.

4.2. Band gap analysis

Band gap analysis of the films deposited under various process conditions has shown very interesting and informative results not only for obtaining the qualitative assessment but also in using them in the appropriate multilayer devices. Films prepared under certain deposition conditions have shown some tailoring in the absorption edges similar to indirect band gaps. Fig. 6 shows a plot of the absorption coefficient, α vs. energy (in eV) for a film deposited under higher substrate temperature of 350 °C, oxygen pressure of 2×10^{-4} mbar and the rate of evaporation of 1.0 nm/s.

As it can be seen from this plot, there are two distinct regions showing the features of both the direct and indirect band gaps. In order to determine the band gaps precisely, the following equation has been used with

respect to the appropriate energy dependence. It is well known that for high absorbing region where α exceeds 10^4 cm^{-1} , α obeys

$$\alpha = B(h\nu - E_{\text{opt}})^r/h\nu \quad (4)$$

where E_{opt} is the optical band gap energy and B is a constant, and $r=1/2, 3/2, 2, 3$ depending upon the type of the electronic transitions. For allowed direct transitions $r=1/2$ while $r=3/2$ for forbidden direct transition. For allowed indirect transition $r=2$ and for forbidden indirect transition $r=3$. The range within which this equation is valid is very small and hence sometimes it becomes too difficult to determine the exact value of the exponent r .

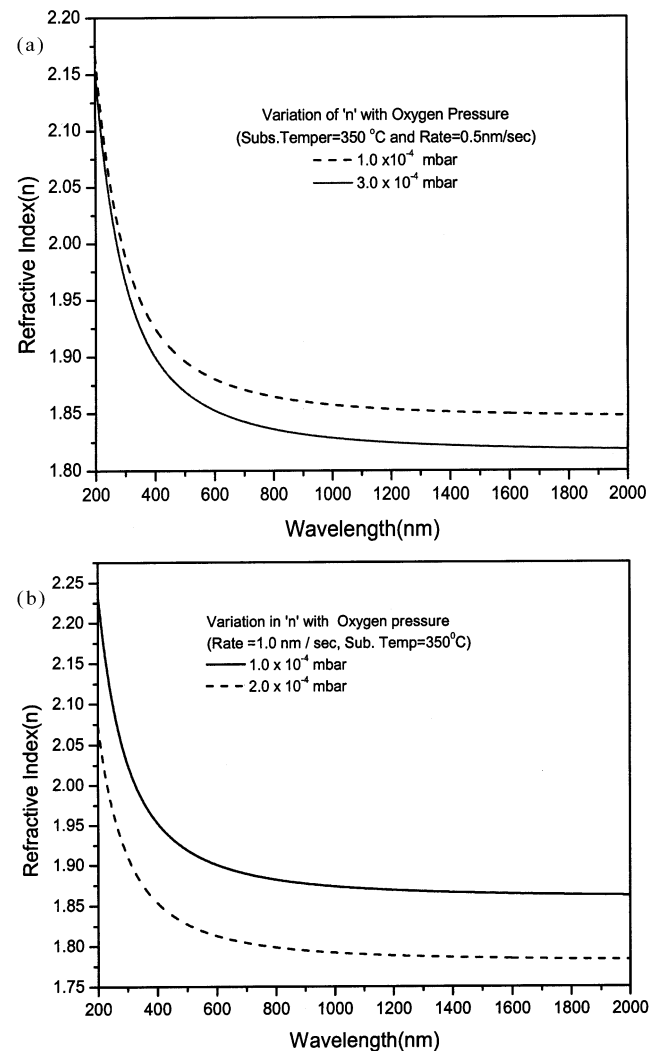


Fig. 4. Spectral variation of refractive index with respect to oxygen pressures (a) at substrate temperature of 350 °C and deposition rate of 0.5 nm/s and (b) at substrate temperature of 350 °C and deposition rate of 1.0 nm/s.

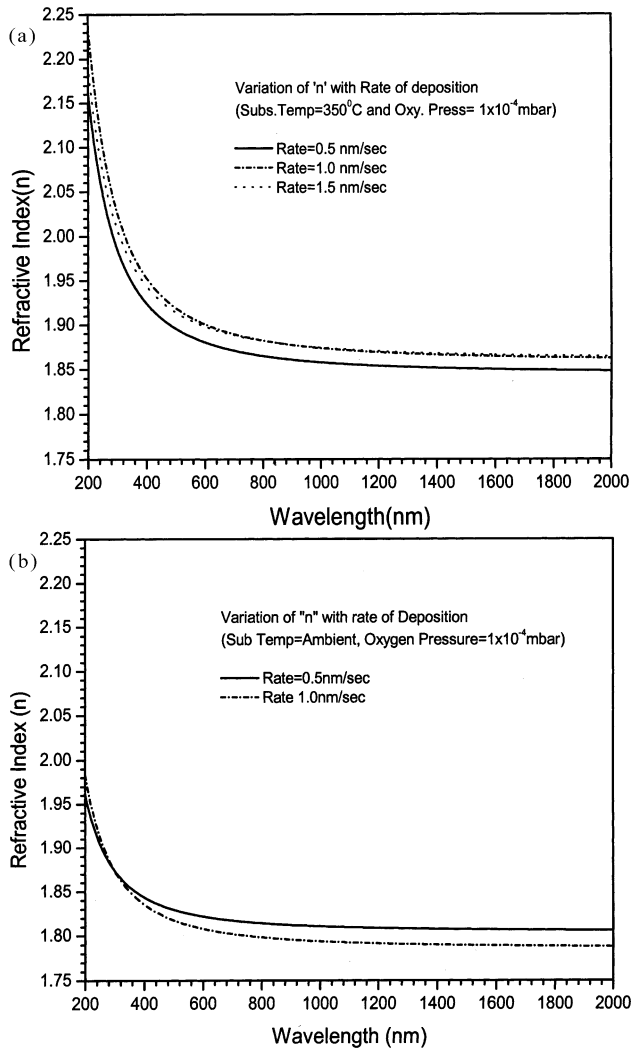


Fig. 5. Spectral variation of refractive index with rate of deposition at (a) substrate temperature of 350 °C and oxygen pressure of 1×10^{-4} mbar and (b) at ambient substrate temperature and oxygen pressure of 1×10^{-4} mbar.

The simplest way to deduce the type of transition is to examine the value of r , which relates $h\nu$ to α^r with a linear relationship. As shown in Fig. 7a and b, in the respective small energy ranges, the linear dependence of $\alpha^{1/2}$ and α^2 on $h\nu$ have been identified and plotted in the graphs. For this sample the direct band gap is 5.65 eV and the value of the indirect band gap is 5.07 eV. During the course of our process-optimizing studies, it was noticed that under several distinct parametric conditions, mostly direct transitions have been observed in the band gaps. One noteworthy observation is the substrate temperature dependence of these band gaps during preparation. It was quite distinctly noticed that films prepared at lower substrate temperatures showed higher band gaps. One of such results has been depicted in Fig. 8a. It can be seen from this plot that while other

parameters being the same ($R=1.5$ nm/s and $O_2=1 \times 10^{-4}$ mbar), the film prepared at ambient substrate temperature has a higher band gap of 6.3 eV than a film prepared at a substrate temperature of 350 °C having a smaller band gap of 5.86 eV. It is interesting to note that there is a strong interdependence of deposition parameters in achieving a wide range of optical properties and band gaps in these films. Fig. 8b shows that a different rate of deposition (1 nm/s) can give rise to a higher band gap value (6.36 eV) even on a slightly heated substrate (70 °C). At this deposition rate, the films deposited under the substrate temperature of 250 °C have shown band gap value of 5.37 eV, which is much smaller than the film deposited at higher rate (1.5 nm/s) and higher substrate temperature (350 °C) (as shown in Fig. 8a). During our investigations, we could notice an excellent microstructural compatibility between Gd_2O_3 and SiO_2 films deposited at the substrate temperature of 70 °C, which is very close to ambient values. Scanning probe viscoelasticity measurements have indicated a similar type of matching surface stiffness property in these films at this temperature condition.

Such deposition conditions are also highly favourable while making filters and coatings on metallic, polymer and plastic substrates. All these studies indicate that contrary to other oxide materials, which invariably need higher substrate temperature for achieving high quality and stable films, gadolinium oxide can yield a stable film structure at lower and even at ambient conditions. The more detailed aspects of these stability criteria are presented in the following sections. Fig. 9 depicts the band gaps of the films deposited at ambient substrate temperature and at two different rates. As it can be seen

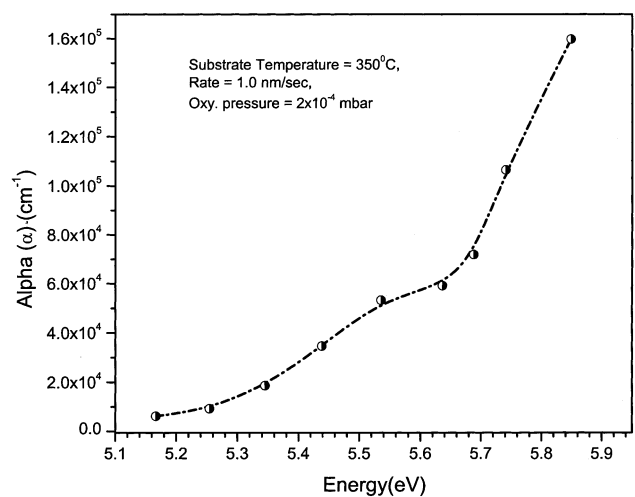


Fig. 6. Absorption co-efficient of Gd_2O_3 film deposited under substrate temperature of 350 °C, deposition rate of 1.0 nm/s and oxygen pressure of 2×10^{-4} mbar indicating the presence of both direct and indirect band gaps.

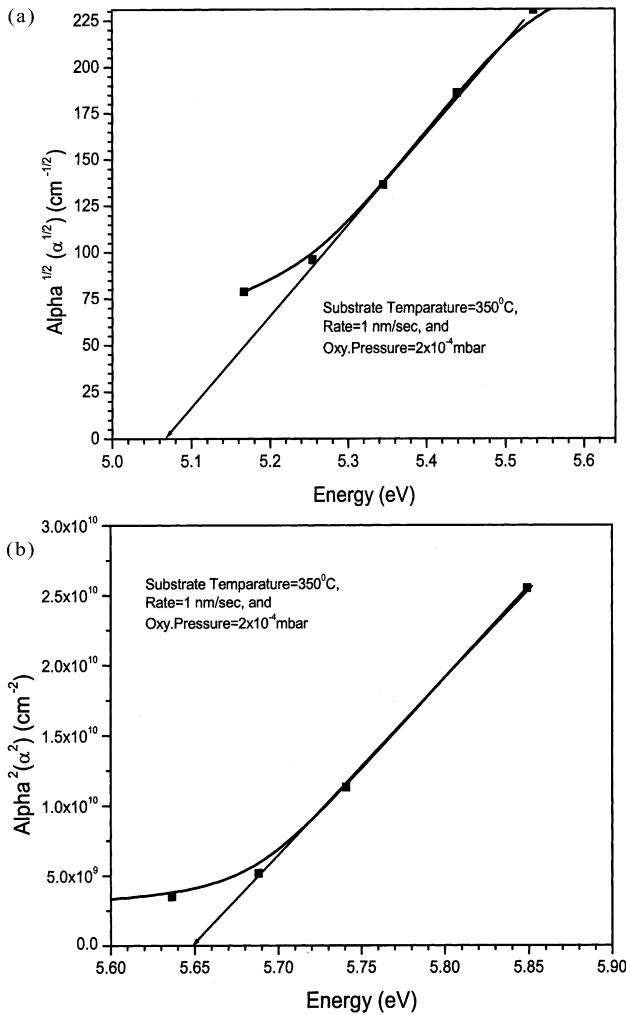


Fig. 7. Graphical determination of optical band gaps (a) Indirect band gap, (b) Direct band gap of Gadolinium oxide thin film deposited at substrate temperature of 350 °C, deposition rate of 1.0 nm/s and the oxygen pressure of 2×10^{-4} mbar.

from this figure, the lower rate of 0.5 nm/s has yielded a higher band gap value of 6.32 eV under ambient substrate temperature condition.

5. Analysis by atomic force microscopy

The surface properties and topography of the thin film samples have been investigated by a multimode scanning probe microscope system of NT-MDT’s Solver P-47H using its AFM head. The capabilities with this scanning head are related to the measurement of surface topography, hardness distribution, friction forces, adhesion characteristics, viscoelasticity, electrical potential conductivity and surface capacitance [26,27]. In the present studies all the AFM measurements were carried out in ambient environment using contact mode operation. Silicon cantilevers having a typical spring constant of 0.6 N/m and resonant frequency of 75 kHz were

used for both topographic and viscoelastic measurements. Gadolinium oxide films deposited under various process parameters have shown a variety of interesting topographic and other microstructural properties. In this work, some of the very prominent aspects of the film properties are presented. Viscoelasticity and long-term spectral stability measurements have established a very good correlation in the experimental results.

5.1. Topographic measurements

Using this measurement sample films prepared under two different temperatures have been characterized for their topographies. Fig. 10a and b portray the surface topographies of Gadolinium oxide thin films deposited at substrate temperatures of 350 °C and 70 °C, respectively. As it can be seen from the measurements, the

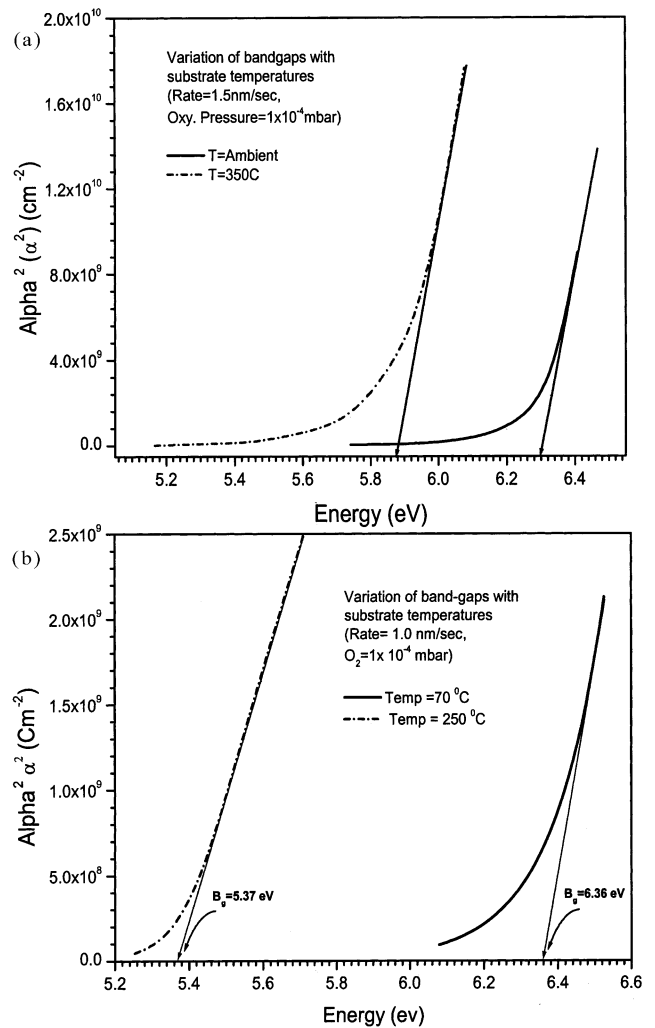


Fig. 8. Plot of α^2 with photon energy for thin films deposited (a) at substrate temperatures of ambient and 350 °C with deposition rate of 1.5 nm/s and (b) at substrate temperatures of 70 °C and 250 °C but with a different rate of 1 nm/s.

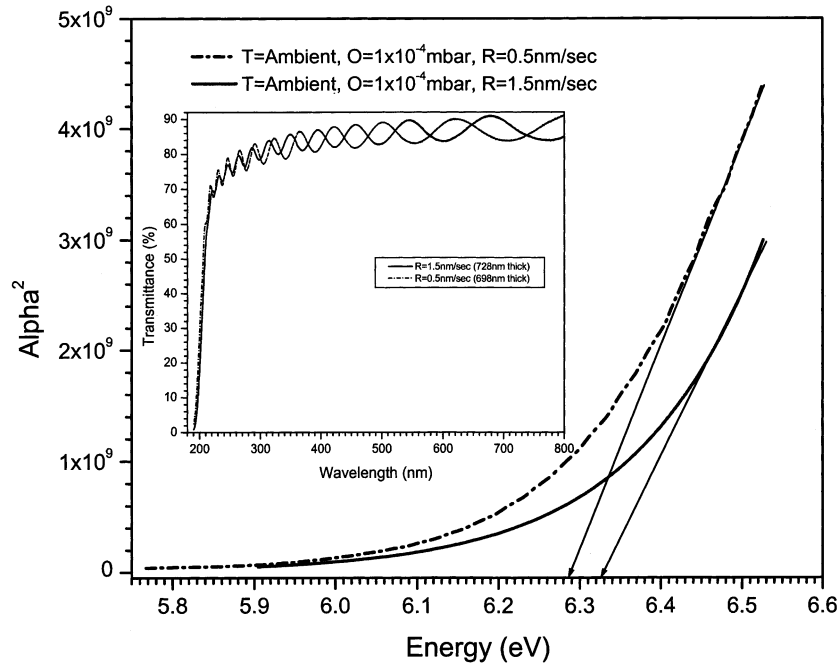


Fig. 9. Plot of α^2 with photon energy for two different thin films deposited at rate of deposition of 0.5 nm/s and 1.0 nm/s, respectively. The films were deposited at ambient conditions.

film deposited at lower substrate temperature is dominated by large grain structures with an average roughness value of 12.63 nm. The root mean square (RMS) value of the roughness for such a sample is 16.25 nm. However, the film deposited at higher substrate temperatures has shown more regular and small features in the topography. It has an overall roughness value of 5.76 nm and RMS value of 7.2 nm. This clearly indicates improved topographic properties of the films deposited at elevated temperature at the expense of smaller optical band gaps. Appearance of smaller grain size at higher

temperatures may be attributed to favorable adatom mobility in yielding better film density and index. The roughness values obtained by these measurements are comparable with the information obtained through ellipsometric modeling.

5.2. Force modulation (Local Viscoelasticity Imaging) results

This mode is usually done simultaneously with conventional AFM topographic imaging and helps in iden-

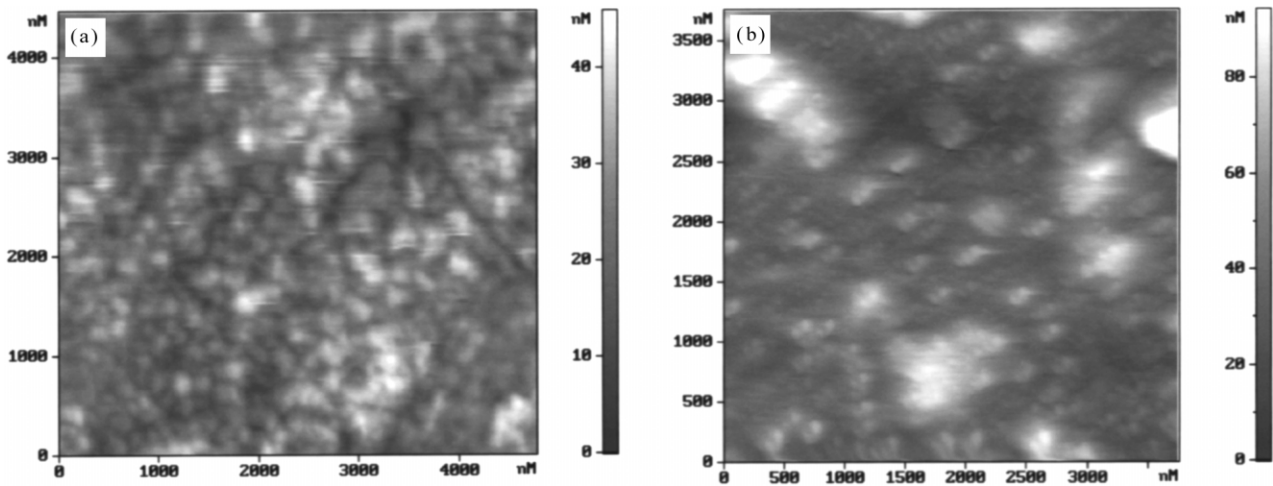


Fig. 10. AFM scans of Gd_2O_3 films deposited at (a) 350 °C and (b) 70 °C showing two-dimensional topographic variations. Corresponding roughness values are 5.76 nm and 12.63 nm, respectively.

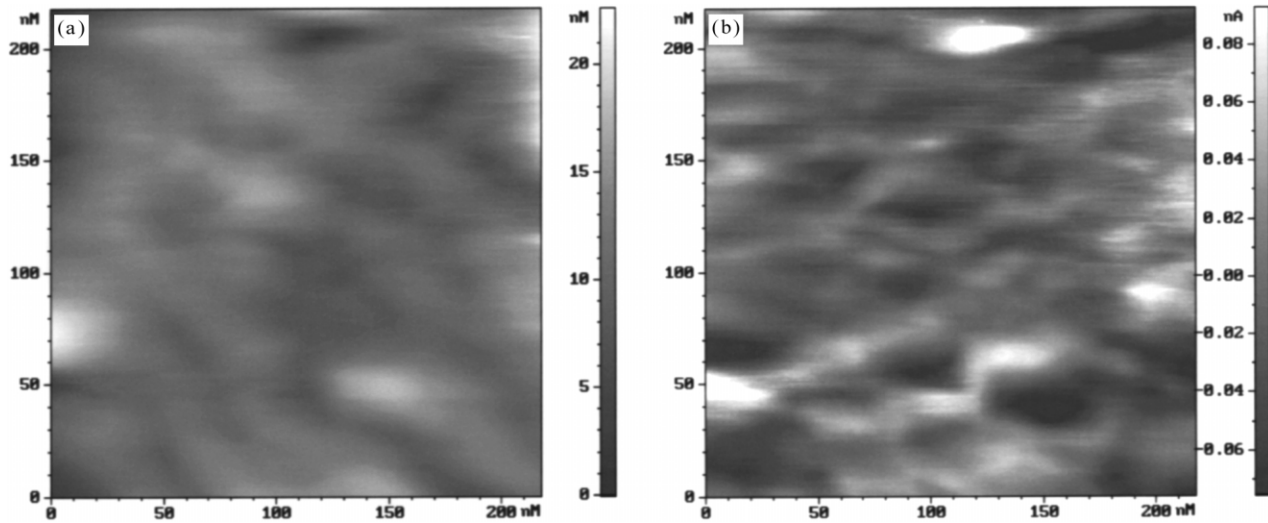


Fig. 11. Two-dimensional (a) Topography and (b) Force modulation AFM images of Gd_2O_3 film deposited at substrate temperature of 70°C , deposition rate of 1.0 nm/s and oxygen pressure of $1 \times 10^{-4}\text{ mbar}$.

tifying and mapping the differences in surface stiffness or elasticity. Force modulation technique is particularly useful for detecting soft and stiff areas on substrates or films, which exhibit overall uniform topography [28–30]. With the force modulation technique, the probe or the cantilever usually moves with a small vertical (z) oscillation (modulation), which is significantly faster than the scan-rate. It has important applications where surface features must be differentiated, and also in investigative studies of relative surface elasticity. These techniques use a variety of surface properties to differentiate among different component materials on heterogeneous surfaces.

The force on the sample is modulated about the set point scanning force such that the average force on the sample remains equal to that in simple contact mode. When the probe is modulated into contact with a sample, the sample surface resists the oscillation and the cantilever bends. Under the same applied force, a stiff area on the sample will deform less than a soft area; i.e. stiffer areas put up greater resistance to the vertical oscillation and consequently, greater bending of the cantilever. The variation in cantilever deflection amplitude at the frequency of modulation is a measure of the relative stiffness of the surface. Topographical information (DC, or non-oscillatory deflection) is collected

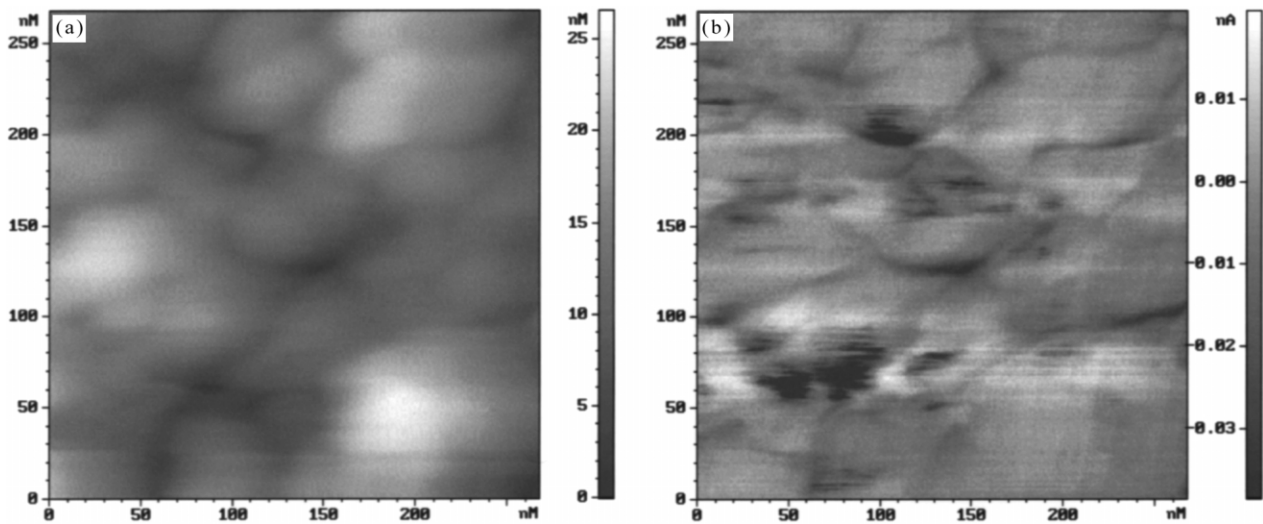


Fig. 12. Two-dimensional (a) Topography and (b) Force modulation images of Gd_2O_3 film deposited at a substrate temperature of 70°C , deposition rate of 2.0 nm/s and oxygen pressure of $1 \times 10^{-4}\text{ mbar}$.

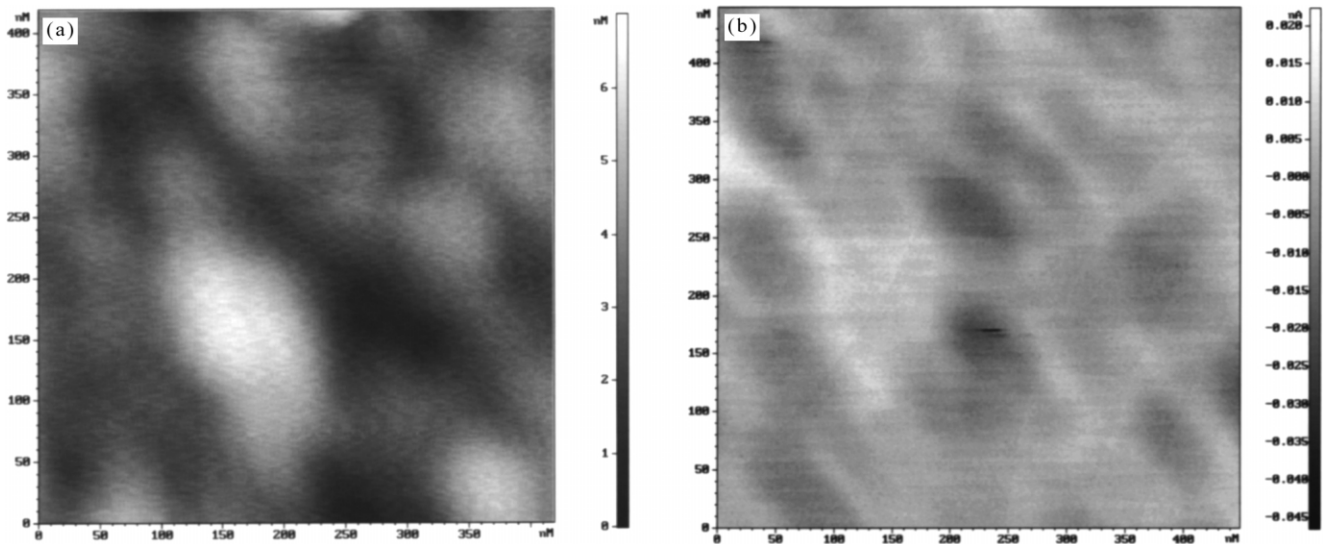


Fig. 13. Two-dimensional (a) Topography and (b) Force modulation images of $\text{Gd}_2\text{O}_3 + \text{SiO}_2$ multilayer reflecting filter developed for KrF (248 nm) laser applications. The surface viscoelastic image shows a uniform contrast over the surface implying an appreciable multilayer stability.

simultaneously with the force modulation data (AC, or oscillatory deflection).

The force modulation images as depicted in Figs. 11b and Fig. 12b clearly differentiates the stiffer black area from the softer white zones and with some regularities in their positions. As it has been shown in Figs. 11a and 12a, the topographical images hint at their presences only. This information is extremely useful when developing a stable multilayer structure combining two or more different thin film materials (such as $\text{Gd}_2\text{O}_3 + \text{SiO}_2$ multilayers). One can achieve a better stability in the multilayer device by choosing appropriate properties in surface elasticity in the component films. In the present case, appropriate deposition parameters for Gd_2O_3 films have chosen ($T=70^\circ\text{C}$, $R=0.8\text{ nm/s}$, $\text{O}_2=0.8\times 10^{-4}\text{ mbar}$) so that its viscoelasticity has a good match with that of SiO_2 films ($T=70^\circ\text{C}$, $R=1.0\text{ nm/s}$, $\text{O}_2=1.0\times 10^{-4}\text{ mbar}$). A surface with uniform viscoelastic property shows minimum contrast variation in the acquired force modulation image. In fact this aspect has been experimentally verified with the AFM measurement results of 25-layer 248 nm (KrF) reflecting filter as shown in Fig. 13a and b. The viscoelastic imaging of such a multilayer (Fig. 13b) has shown a uniform elasticity over the multilayer surface, which has ultimately demonstrated a very stable spectral characteristic in our spectrophotometric measurements.

6. Development of multilayer UV laser filters

Using gadolinium oxide (Gd_2O_3) (Substrate temperature: 70°C , Rate: 0.8 nm/s , Oxygen partial pressure: $0.8\times 10^{-4}\text{ mbar}$) as high index material along with

silicon dioxide (SiO_2) (Substrate Temperature: 70°C , Rate: 1.0 nm/s , Oxygen partial pressure: $1.0\times 10^{-4}\text{ mbar}$) as the low index counterpart, several multilayer reflectors and filters have been successfully developed and tested for various laser applications. Out of these precision multilayer devices, experimental and computed spectral characteristics of four reflectors have been presented in Figs. 14–17, which have been developed for Nd-Yag-III (355 nm), KrF (248 nm), KrCl (222 nm) and ArF (193 nm) laser applications, respectively. Amongst these, the reflection filters for KrF, KrCl and

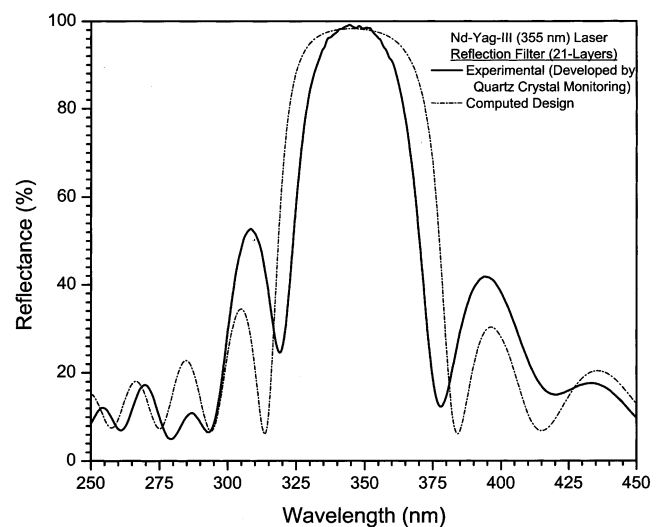


Fig. 14. Experimental and computed reflection spectra of Nd-YAG-III (355 nm) reflection filter, consisting of 21 alternative layers of Gd_2O_3 and SiO_2 . The quarterwave design adopted here is $(\text{HL})^{10}\text{H}$, where H is Gd_2O_3 and L is SiO_2 .

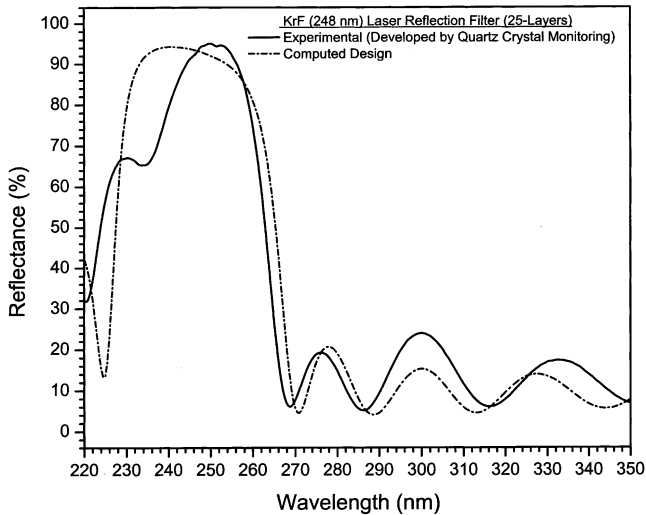


Fig. 15. Experimental and computed reflection spectra of 248 nm reflection filter for KrF Laser, consisting of 25 alternative layers of Gd_2O_3 and SiO_2 (Stack design: $(HL)^{12}$ 0.7 H).

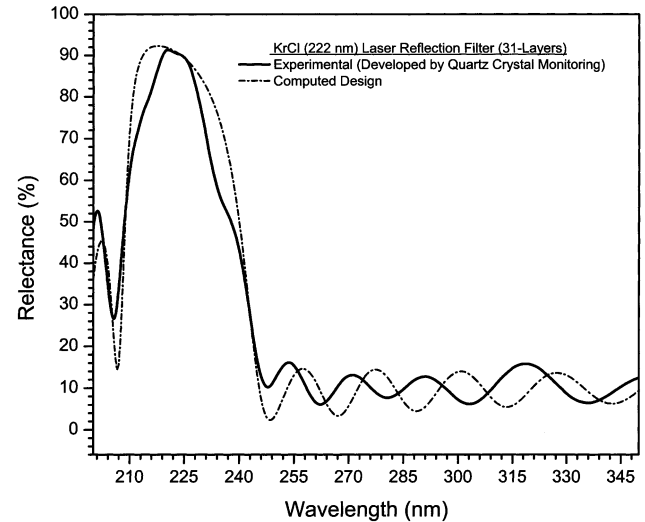


Fig. 16. Experimental and computed reflection spectra of 222 nm reflection filter for KrCl Laser, consisting of 31 alternative layers of Gd_2O_3 and SiO_2 (Stack design: $(HL)^{15}$ 0.3 H).

ArF lasers are highly challenging, and demonstrate the usefulness of this material for deep ultraviolet applications. We have used 41 alternative layers of Gd_2O_3 and SiO_2 to achieve the required reflectance spectra for ArF (193 nm) laser application and the experimental and computed characteristics are shown in Fig. 17. The last layer is chosen as half of a quarterwave to reduce the ripples in the pass band as per the experimental requirements. For KrCl (222 nm) and KrF (248 nm)-lasers reflecting filters, 31 and 25 layers of alternative Gd_2O_3 and SiO_2 have been used, respectively. The last layers (Gd_2O_3) in these designs were appropriately chosen to minimize the ripples in the pass band to the desired limit. For the development of these extreme ultraviolet devices, the quartz crystal monitor XTC/2 has been suitably calibrated using OMS 2000 optical monitor system. The post deposition reflection spectra were recorded using Shimadzu UV3101PC spectrophotometer system fitted with a specular reflection attachment. An integrating sphere accessory in this instrument has been used to record the diffused reflectance values of the developed multilayer filters. It is worth mentioning that in spectrophotometric measurements, transmittance spectra is better calibrated than the reflectance spectra and so also the accuracies. Besides, in Shimadzu 3101pc spectrophotometer, the specular reflectance attachment uses an incidence angle of 5° during the measurement. For such reasons, the experimental $R+T$ of some multilayer devices have slightly exceeded 100% in certain spectral regions due to a small calibration error in the reflectance-measuring mode of the instrument. The differences in the computed and experimental spectral reflectance characteristics of these developed filters can

be attributed to the quartz crystal calibration and monitoring errors in detecting the specified layer thicknesses. Besides, the dispersive complex refractive indices of each sub-layer in the multilayer devices might have differed from each other affecting both the bandwidths as well as amplitudes of the spectral characteristics. Dispersion being more dominant in this lower wavelength region of the spectrum introduces larger errors in the experimental characteristics with respect to their computed values.

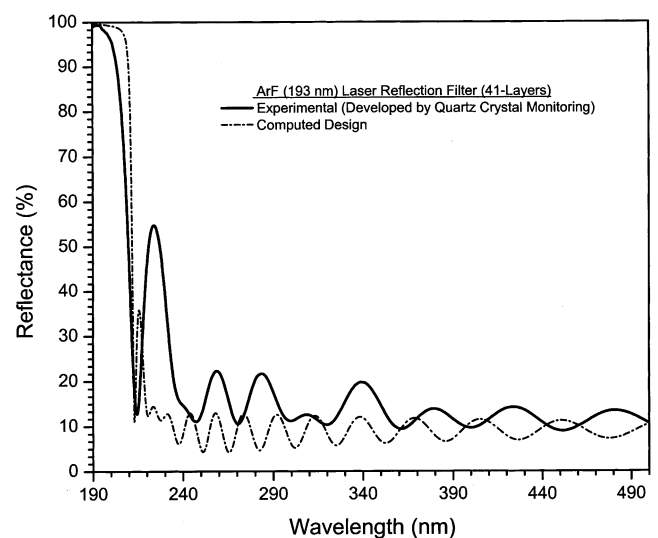


Fig. 17. Experimental and computed reflection spectra of 193 nm reflection filter for ArF Laser, consisting of 41 alternative layers of Gd_2O_3 and SiO_2 (Stack design: $(HL)^{20}$ 0.5 H).

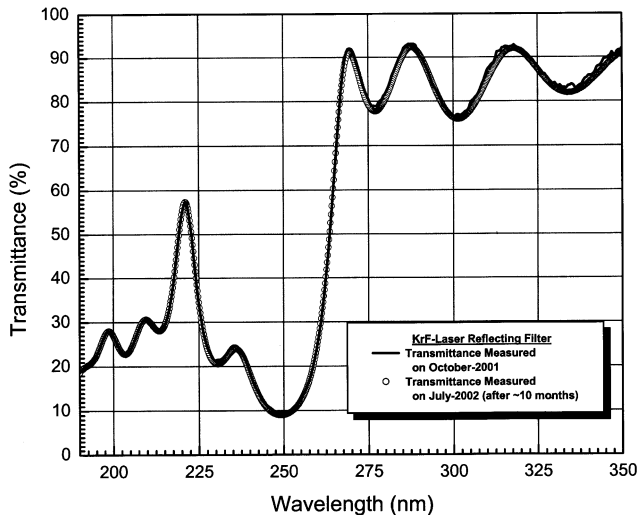


Fig. 18. Spectral transmittance characteristics of 248 nm (KrF) reflection filter measured in October 2001 and then in July 2002; i.e., at a time interval of approximately 10 months after repetitive use with the laser. Both the measurements have shown almost no shift in the spectral characteristic, which indicate a very appropriate multilayer temporal stability.

All these multilayer devices have shown quite stable post-depositional spectral characteristics with respect to aging. The transmittance spectra of KrF (248 nm) reflector measured at an interval of 10 months of use with the laser have been depicted in Fig. 18. Both spectra have shown a very negligible shift in their characteristics implying an extremely good temporal spectral stability with respect to aging. This device is being used effectively for a spectroscopic experiment with a KrF laser system (248 nm) operating at a pulse energy of 400 mJ, pulse width of 25 ns and repetition rate of 100 Hz. Similarly the device developed for Nd-Yag-III laser application (355 nm) has been successfully used in another experiments with the laser pulse energy of 200 mJ, pulse width of 6 ns and a repetition rate of 10 Hz.

7. Conclusions

Optical and microstructural properties of electron beam deposited gadolinium oxide films, a novel lanthanide sesquioxide optical material, have been studied in detail for the application in multilayer optical coatings with our present requirements to the ultraviolet and deep ultraviolet regions. The films have been characterized by phase modulated spectroscopic ellipsometry, multi-mode atomic force microscopy and uv–vis–nir spectrophotometric techniques. Interestingly, the films deposited at lower and ambient substrate temperatures have shown higher band gaps making them attractive for excimer laser applications as well as for a variety of substrate

materials. During our experiments, band gap values have been observed in the range of 6.36 eV for the films deposited under lower values of substrate temperatures. However, films deposited at elevated substrate temperatures have shown smooth topographies with higher values in refractive indices and smaller RMS roughness. Surface viscoelasticity measurements through force modulation AFM technique have shown a near regular distribution of soft and stiff zones on the surfaces of most sample films. Using process optimized films as high index layers several high reflection filters for various ultraviolet laser applications, such as KrCl, KrF, XeF and Nd-YAG-III wavelengths, have been successfully developed and used for our spectroscopic experiments with a high degree of long-term spectral stability and reliability.

References

- [1] N. Kaiser, H. Uhlig, U.B. Schallenberg, B. Anton, U. Kaiser, K. Mann, E. Eva, *Thin Solid Films* 260 (1995) 86.
- [2] F. Rainer, W.H. Lowdermilk, D. Milam, T. Tuttle-Hart, T.L. Lichtenstein, C.K. Carniglia, *Appl. Opt.* 21 (1982) 3685.
- [3] R. Chow, S. Falabella, G.E. Loomis, F. Rainer, C.J. Stolz, M.R. Kozlowski, *Appl. Opt.* 32 (1993) 5567.
- [4] N.K. Sahoo, A.P. Shapiro, *Appl. Opt.* 37 (1998) 698.
- [5] J.A. Dobrowolski, L. Li, *Appl. Opt.* 34 (1995) 2934.
- [6] D. Landheer, J.A. Gupta, G.I. Sproule, J.P. McCaffrey, M.J. Graham, K.-C. Yang, Z.-H. Lu, W.N. Lennard, *J. Electrochem. Soc.* 148 (2001) G29.
- [7] J.A. Gupta, D. Landheer, G.I. Sproule, J.P. McCaffrey, M.J. Graham, K.-C. Yang, Z.-H. Lu, W.N. Lennard, *Appl. Surf. Sci.* 173 (2001) 318.
- [8] F. Tcheliébou, M. Boulouz, A. Boyer, *J. Mater. Res.* 12 (1997) 3260.
- [9] C. Steiner, B. Bolliger, M. Erbudak, *Phys. Rev. B* 62 (2000) R10614.
- [10] A. García-Murillo, C. Le Luyer, C. Garapon, C. Dujardin, E. Bernstein, C. Pedrini, J. Mugnier, *Opt. Mater.* 19 (2002) 161.
- [11] A.A. Dakhel, *J. Opt. A: Pure Appl. Opt.* 3 (2001) 452.
- [12] D. Bhattacharyya, N.K. Sahoo, S. Thakur, N.C. Das, *Thin Solid Films* 360 (2000) 96.
- [13] D. Bhattacharyya, N.K. Sahoo, S. Thakur, N.C. Das, *Appl. Opt.* 40 (2001) 1707.
- [14] R. Swanepoel, *J. Phys. E: Sci. Instrum.* 16 (1983) 1214.
- [15] R. Swanepoel, *J. Phys. E: Sci. Instrum.* 17 (1984) 896.
- [16] B. Drévilion, *Prog. Cryst. Growth. Charac. Mater.* 27 (1993) 1.
- [17] N.K. Sahoo, *Vacuum* 60 (2001) 411.
- [18] G. Parjadis de Larivière, J.M. Frigerio, J. Rivory, F. Abelès, *Appl. Opt.* 31 (1992) 6056.
- [19] J.C. Charmet, P.G. de Gennes, *J. Opt. Soc. Am.* 73 (1983) 1777.
- [20] A.V. Tikhonravov, M.K. Trubetskov, A.V. Krasilnikova, *Appl. Opt.* 37 (1998) 5902.
- [21] A.V. Tikhonravov, M.K. Trubetskov, B.T. Sullivan, J.A. Dobrowolski, *Appl. Opt.* 36 (1997) 7188.
- [22] D.E. Aspnes, *Thin Solid Films* 89 (1982) 249.
- [23] N.K. Sahoo, A.P. Shapiro, *Appl. Opt.* 37 (1998) 8043.
- [24] P. Chindaudom, K. Vedam, in: K. Vedam (Ed.), *Optical Characterization of Inhomogeneous Transparent Thin Films on*

- Transparent Substrates, 19, Academic Press, New York, 1994, p. 191.
- [25] S.Y. Kim, *Opt. Eng.* 32 (1993) 88.
- [26] G. Binnig, C.F. Quate, Ch. Gerber, *Phys. Rev. Lett.* 56 (1986) 930.
- [27] G. Meyer, N.M. Amer, *Appl. Phys. Lett.* 57 (1990) 2089.
- [28] S.A. Syed Asif, K.J. Wahl, R.J. Colton, *Rev. Sci. Instr.* 70 (1999) 2408.
- [29] K.J. Wahl, S.V. Stepnowski, W.N. Unertl, *Tribol. Lett.* 5 (1998) 103.
- [30] R. Resch, G. Friedbacher, M. Grasserbauer, T. Kanninen, S. Lindroos, M. Leskelä, L. Niinistö, *Appl. Surf. Sci.* 120 (1997) 51.